length x_e, which a constant velocity missile would travel in time t:

$$x_e = -(u/d)t = (e^{C_D{}^*x} - 1)/C_D{}^* \quad [8]$$

Effective lengths were computed for the data of this report, and revised versions of Eqs. [2b] and [5b] obtained

$$(r + 1.2)^3 = x_e/7.9 \quad [9]$$

$$r^3 = (x_e - 415)/11.1 \quad [10]$$

Once again one sees the importance of knowing the proper form of the wake growth. From the coefficient of Eq. [10] a better value of C_D may be calculated by means of the Lees-Hromas theory. This value, 1.2, is 20% higher than the true value. Since K is certainly not any better known than 20%, this is a very encouraging verification of the Lees-Hromas theory.

Summary

1) Experimental determination of the exponential coefficient in the growth law for a turbulent wake is very difficult, if not impossible.

2) If use is made of the theoretically predicted value of this coefficient, the existence of two distinct regions of growth ($x < 200$, $x > 200$) is shown by the experimental data.

3) Although the Slattery and Clay data indicate a scale effect for $\frac{1}{4}$- and $\frac{1}{2}$- in. spheres, the authors' $\frac{1}{8}$- and $\frac{1}{4}$-in. sphere data indicate at most a much weaker scale effect.

4) It is important to fit the data with the proper algebraic expression of the theoretical growth law, i.e., $r^3 = bx + c$.

5) If the effect of sphere deceleration is assumed to be described by a quasi-steady state transformation, the coefficient b for the far wake is well predicted by the Lees-Hromas theory.

References

1 Birkhoff, G. and Zarantonello, E. H., *Jets, Wakes and Cavities* (Academic Press, New York, 1957).

2 Morton, B. R., "On a momentum-mass flux diagram for turbulent jets, plumes and wakes," J. Fluid Mech. **10**, Part 1, 101–112 (1961).

3 Lees, L. and Hromas, L., "Turbulent diffusion in the wake of a blunt-nosed body at hypersonic speeds," Aeronaut. Dept. Rept. 50, Space Technology Labs. Inc. (July 1961); also Inst. Aerospace Sci. Paper 62-71.

4 Cooper, R. D. and Lutzky, M., "Exploratory investigation of the turbulent wakes behind bluff bodies," David W. Taylor Model Basin Rept. 963 (October 1955).

5 Billerbeck, W. J., Jr., "Empirical equation for the wake-spreading limits behind three-dimensional bodies," J. Aerospace Sci. **27**, 640 (1960).

6 Dana, T. A. and Short, W. W., "Experimental study of hypersonic turbulent wakes," Convair, San Diego, Calif., ZPh-103 (May 1961).

7 Slattery, R. E. and Clay, W. G., "Width of the turbulent trail behind a hypervelocity sphere," Phys. Fluids **4**, 1199–1201 (1961).

8 Braun, W. F., "The free flight aerodynamics range," Aberdeen Proving Ground BRL R 1048 (July 1958).

FEBRUARY 1963 AIAA JOURNAL VOL. 1, NO. 2

Compressible Free Shear Layer with Finite Initial Thickness

M. Richard Denison* and Eric Baum†

Electro-Optical Systems Inc., Pasadena, Calif.

The momentum equation was uncoupled from the other conservation equations for the case of a finite initial profile in a laminar free shear layer. The equation was solved numerically, in the Crocco coordinate system, using an implicit finite difference method. Profiles of velocity and shear function were obtained as a function of streamwise distance. The initial profiles as the flow separates from the rear of the body correspond to the Blasius profile in transformed coordinates. For large distances downstream, the profiles approach the Chapman distribution, corresponding to the case of zero initial free shear layer thickness. The effect of these results on calculations of base pressure and wake angle is discussed. A method for the calculation of finite chemical kinetic effects on the profiles of temperature and chemical composition in the free shear layer with finite initial thickness is outlined.

Nomenclature

C = Chapman-Rubesin parameter, see Eq. (7)
F = shear function, see Eq. (8)
F_0 = initial shear function
F_w = initial shear function at body surface
F^* = F/F_w
P = pressure
r_0 = distance from axis of symmetry to body surface or dividing streamline
S = transformed distance parameter, see Eq. (4)
S_b = parameter S evaluated for body
S^* = $SCF_w{}^2$
u = component of velocity along dividing streamline
u^* = u/u_e
U = $u^*(3S^*)^{-1/3}$
v = component of velocity perpendicular to dividing streamline
$\bar{v}$ = transformed velocity component, see Eq. (7)
x = distance along dividing streamline from base of body
y = distance normal to dividing streamline
Y = normal distance parameter, see Eq. (3)
η = normal distance parameter for similar solutions, see Eq. (9)
μ = viscosity
ψ = stream function

Subscripts

D = dividing streamline conditions
e = conditions at outer edge of free shear layer

Presented at the IAS Summer Meeting, Hypersonics II (Heat Transfer) Session, Los Angeles, June 19–22, 1962. Received May 11, 1962; revision received November 26, 1962. This work was sponsored by the Advanced Research Projects Agency, Washington, D.C., under ARPA Order 203-61, monitored by the Army Ordnance Missile Command, Huntsville, Ala., under Contract DA-04-495-ORD-3245.

* Manager, Fluid Dynamics and Plasma Propulsion Department.
† Senior Scientist.

I. Introduction

THE length of trail behind a body, defined by observables such as electron density and radiation intensity, is de-

termined by the diffusion and recombination processes in the wake. Since the wake is very complex from the standpoint of fluid mechanics, many subdivisions of the wake can be defined. A crude description consists of the outer wake, the inner wake, and the base flow. The outer wake contains velocity, temperature, and species gradients due to the varied origin and history of its streamlines. The cooling of this outer wake has been studied by Feldman.[1] The inner wake is the viscous region near the axis downstream of the "neck" of the wake. When this region is turbulent, it can completely swallow the outer wake before cooling of the outer wake takes place. This region has been studied recently by Lees and Hromas[2] under the assumption of thermodynamic equilibrium.

The base flow region extends from the base of the body to the neck of the wake. This region was studied by Chapman[3] primarily for the purpose of determining the base pressure because of its influence on drag. A sketch of this region is shown in Fig. 1. The layer begins with some finite thickness due to the upstream flow over the body. The dividing streamline separates those streamlines which continue downstream through the neck of the wake from those which turn back and recirculate.

Chapman[3] studied the case in which the initial boundary layer thickness is zero in order to simplify the mathematics. It turns out in this case that a similar solution to the equations of motion is obtained; that is, the flow field can be determined in terms of one space variable which contains both physical coordinates. The solution of Chapman actually applies only to that portion of the base flow in which recirculating mass is being entrained by the shear stresses of the outer flow. In order to determine the base pressure, Chapman assumed that the recompression region where the recirculating flow turns back is small in extent. He then assumed that the total pressure on the dividing streamline is equal to the static pressure behind the trailing shock. This assumption plus the analysis of the inviscid flow outside the mixing region serves to determine the base pressure. Although there has been some controversy recently as to the stability of this model its success in predicting base pressure makes it appear reasonable.

The purpose of the present investigation is to improve upon the available base flow calculations in order to obtain more realistic initial conditions for analyses of the downstream wake such as that of Lees and Hromas.[2] The present investigation is of a laminar base flow. Lees and Hromas point out that for a considerable range of Reynolds numbers and Mach numbers of interest a laminar base flow with a turbulent inner wake downstream of the neck is possible. This paper is concerned with the investigation of the influence on the base flow of two effects which have not heretofore been considered quantitatively. The body of this paper covers an analysis of the shear layer flow field when an initial (Blasius) velocity profile exists on the body. An appendix outlines an analysis of the influence of finite chemical rates in the free shear layer.

II. Conservation Equations

The coordinate system as illustrated in Fig. 1 is distance along the dividing streamline and normal to it. The distance r_0 is measured from the centerline for axisymmetric flow. When this distance is large compared to the thickness of the mixing layer, the continuity and momentum equations are as follows:

Continuity

$$\frac{\partial}{\partial x}(\rho u r_0^k) + \frac{\partial}{\partial y}(\rho v r_0^k) = 0 \tag{1}$$

Momentum

$$\rho\left(u\frac{\partial u}{\partial x} + v\frac{\partial u}{\partial y}\right) = \frac{\partial}{\partial y}\left(\mu\frac{\partial u}{\partial y}\right) - \frac{dP}{dx} \tag{2}$$

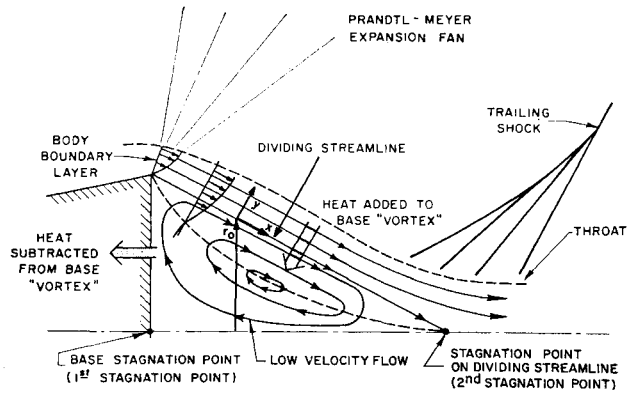

Fig. 1 Base flow region

where $k = 0$ for two-dimensional flow, $k = 1$ for axisymmetric flow. Transformations like those of Howarth and Levy are introduced

$$Y = \rho_e u_e r_0^k \int_0^y (\rho/\rho_e)dy \tag{3}$$

$$S = \int_0^x \rho_e u_e \mu_e r_0^{2k} dx \tag{4}$$

(measured from point of separation).

The stream function is defined as

$$\partial\psi/\partial y = \rho u r_0^k \tag{5}$$

$$\partial\psi/\partial x = -\rho v r_0^k \tag{6}$$

Use of these relations in the momentum equation yields

$$\frac{u}{u_e}\frac{\partial u/u_e}{\partial S} + \frac{\tilde{v}}{u_e}\frac{\partial u/u_e}{\partial Y} - \frac{\partial}{\partial Y}\left(C\frac{\partial u/u_e}{\partial Y}\right) = -\frac{dP}{dS}\frac{1}{\rho_e u_e^2}\left[\frac{\rho_e}{\rho} - \left(\frac{u}{u_e}\right)^2\right] \tag{7}$$

where

$$\tilde{v}/u_e = -(\partial\psi/\partial S)_Y \qquad c = \rho\mu/\rho_e\mu_e$$

which will be assumed constant. The term involving the direct effect of the pressure gradient in Eq. (7) can be neglected for hypersonic boundary layers by the arguments of Lees[4] and Moore.[5] For the shear layer the pressure gradient will be negligible in most of the region anyway. In this way the momentum equation is completely uncoupled from the energy and species continuity equations. Hence, it can be solved separately. The energy and species equations can be solved later based on the resulting velocity distribution. Finite kinetics can also be included.

A further transformation to the Crocco coordinate systems proves convenient for numerical calculations. In order to put the momentum equation in this form, it is solved for $\tilde{v}/u_e$, differentiated with respect to Y, and use is made of continuity (or the definition of the stream function) to yield

$$\left(\frac{u}{u_e}\right)\frac{\partial F}{\partial CS} = F^2\frac{\partial^2 F}{\partial(u/u_e)^2} \tag{8}$$

where

$$F = (\partial/\partial Y)(u/u_e)$$

III. Universal Form of Solution

The momentum equation, Eq. (7), also applies to the boundary layer on the body if S represents an integral measured from the nose of the body. The value of this integral carried all the way from the nose to the base of the body will be de-

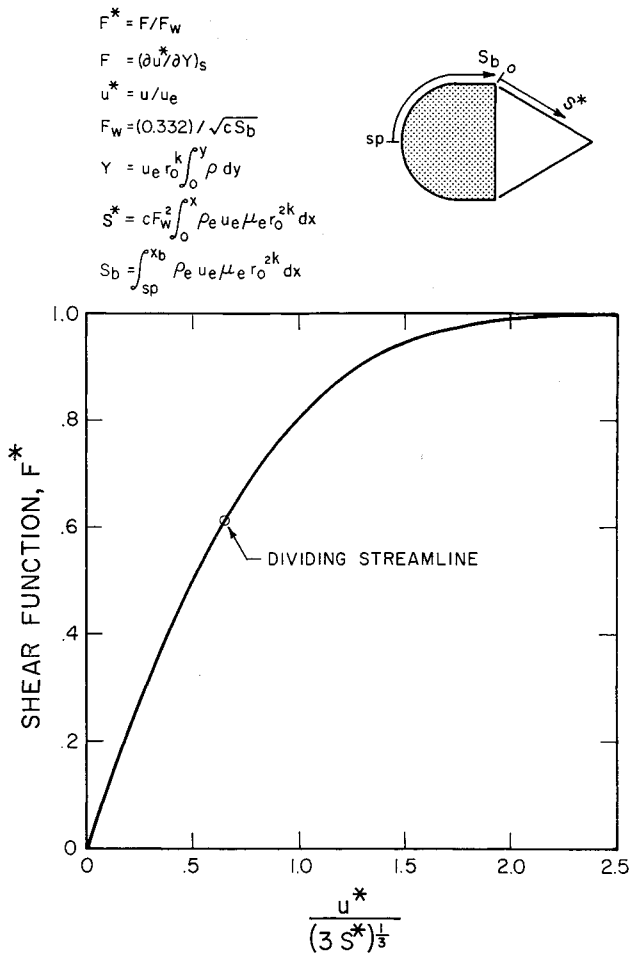

Fig. 2 Solution to the momentum equation for small S^*

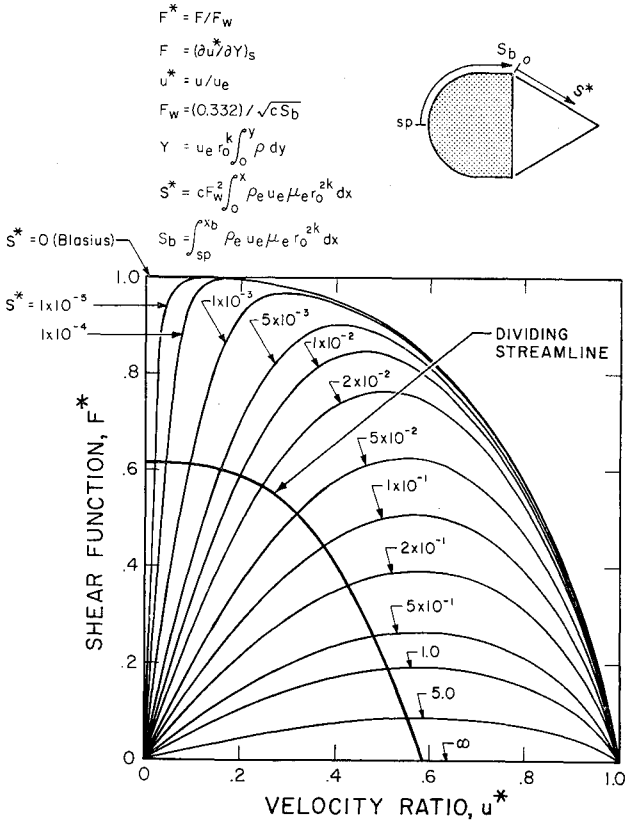

Fig. 3 Shear function profiles emphasizing initial distribution

noted S_b. The velocity distribution at the base of the body is given in the form of a similar solution for several sets of boundary conditions. The one of immediate interest is the axisymmetric or two-dimensional body without blowing, with the velocity distribution given by the familiar Blasius solution,[4] of the form

$$\frac{u}{u_e} = f'(\eta) \qquad \eta = \frac{Y}{\sqrt{2CS_b}} \tag{9}$$

If the expansion about the corner of the body base is rapid, the distribution given by Eq. (9) may be distorted by the direct effect of the pressure gradient on the momentum equation. The effect of the sharpness of the corner on the solutions of Eq. (8) should be investigated further.

When the flow does not turn sharply at the point of separation from the body, the Blasius distribution should still describe the flow at the start of the free shear layer, and Eq. (8) can be reduced to a universal form having one set of solutions applicable to all bodies.

The initial shear distribution, also given by the Blasius solution, has the form

$$\sqrt{2CS_b}\, F_0 = f''(\eta) \tag{10}$$

Hence, the initial shear profile normalized with respect to the wall shear is a universal function of the velocity ratio

$$\frac{F_0}{F_w} = \frac{f''(\eta)}{f''(0)} = F_0^*(u^*) \tag{11}$$

where

$$u^* = u/u_e$$

Then, if the distance coordinate is stretched by defining

$$S^* = CSF_w^2 \tag{12}$$

the momentum equation becomes

$$u^* \frac{\partial F^*}{\partial S^*} = F^{*2} \frac{\partial^2 F^*}{\partial u^{*2}} \tag{13}$$

The boundary conditions which correspond to those of Chapman are

$$F^*(0) = F^*(1) = 0 \qquad S^* > 0 \tag{14}$$

Therefore, with a single universal initial distribution given by Eq. (11), the differential equation, Eq. (13), should yield a single solution, as a function of S^* and u^*. Furthermore, since the boundary conditions imposed are the same as those of Chapman, the solution should approach his results for sufficiently large S^*.

On the dividing streamline $\bar{v}/u_e = -\partial\psi/\partial S = 0$. Hence, from Eq. (7)

$$u_D^* \frac{du_D^*}{dS^*} = F_D^* \left(\frac{\partial F^*}{\partial u^*}\right)_D \tag{15}$$

Once the solution is obtained, u^* vs Y at a given value of S^* can be found by use of

$$YF_w = \int_{u_D^*}^{u^*} \frac{du^*}{F^*} \tag{16}$$

It is immediately apparent that Eq. (15) cannot be used for a numerical solution at the origin, because the value of F_D^* is not known initially and, as will be shown, $(\partial F^*/\partial u^*)_D$ is zero at the origin, making Eq. (15) indeterminate. An independent method of starting the calculation is necessary.

IV. Starting Profile

An indication of the difficulty in starting the solution is obtained by looking ahead to Fig. 3 where the solution is

plotted. The Blasius shear distribution on the body begins at $F^* = 1$ at $u^* = 0$ and goes to zero at $u^* = 1$. In the free shear layer the boundary condition is suddenly changed to $F^* = 0$ at $u^* = 0$. Therefore at $S^* = 0$ the initial distribution goes vertically upward from zero and then follows the Blasius distribution from $F^* = 1$. It can be seen that $(dF^*/du^*) = 0$ at $u^* = 0^+$. This suggests that a starting solution for small S^* should become asymptotic to $F^* = 1$ at a small value of u^* and go through zero at $u^* = 0$.

An equation which is good at small values of S^* can be obtained from Eq. (13) by changing the independent variables from S^* and u^* to S^* and U where

$$U = u^*/(3S^*)^{1/3} \tag{17}$$

This transformation is suggested by the solution of Goldstein[6] who found, for the wake of a flat plate in incompressible flow, that initially the velocity grows as $x^{1/3}$. When the transformation is made the momentum-equation becomes

$$3S^*\left(\frac{\partial F^*}{\partial S^*}\right)_U = U\frac{\partial F^*}{\partial U} + \frac{F^{*2}}{U}\frac{\partial^2 F^*}{\partial U^2} \tag{18}$$

$F^* = F^*(U)$ with the boundary conditions of Eq. (20) satisfies the initial conditions. Therefore, Eq. (18) becomes an ordinary differential equation. The dividing streamline is found from

$$F_D^*(dF^*/dU)_D = U_D^2 \tag{19}$$

The boundary conditions for Eq. (18) are

$$U = 0, \quad F^* = 0 \qquad U \to \infty, \quad F^* \to 1 \tag{20}$$

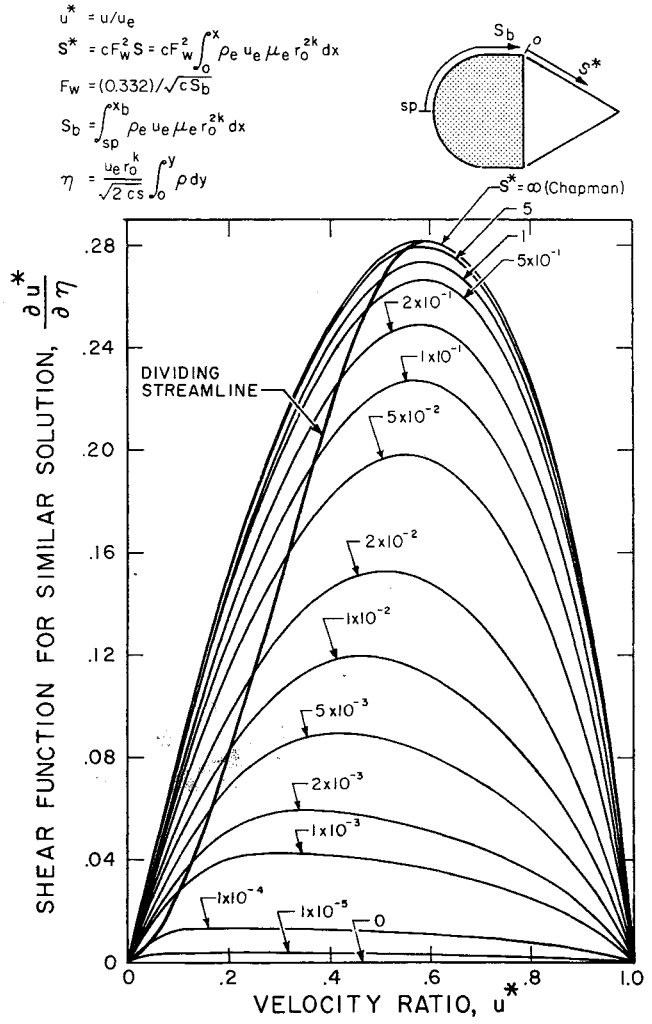

Fig. 4 Shear function profiles showing approach to asymptotic distribution

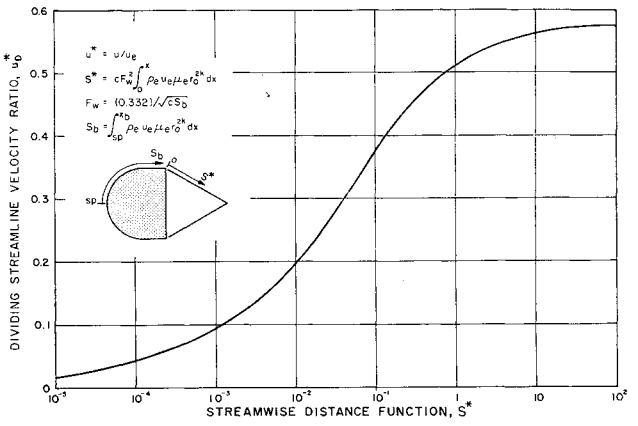

Fig. 5 Velocity on the dividing streamline

The boundary condition at infinity is in the boundary layer sense. For a given value of U when S^* is small u^* will be small. Eq. (18) with these boundary conditions was solved numerically by iteration assuming various values of the slope at the origin until F^* approached unity at large U. The solution is plotted in Fig. 2. The dividing streamline was found by use of Eq. (19).

V. Numerical Method

An attempt was made to use the method of Dorodnitsyn[7] to compute the profile. Because of the shape of the shear profile at small S^* it was found, however, that a very high degree polynomial was required in order to fit the initial

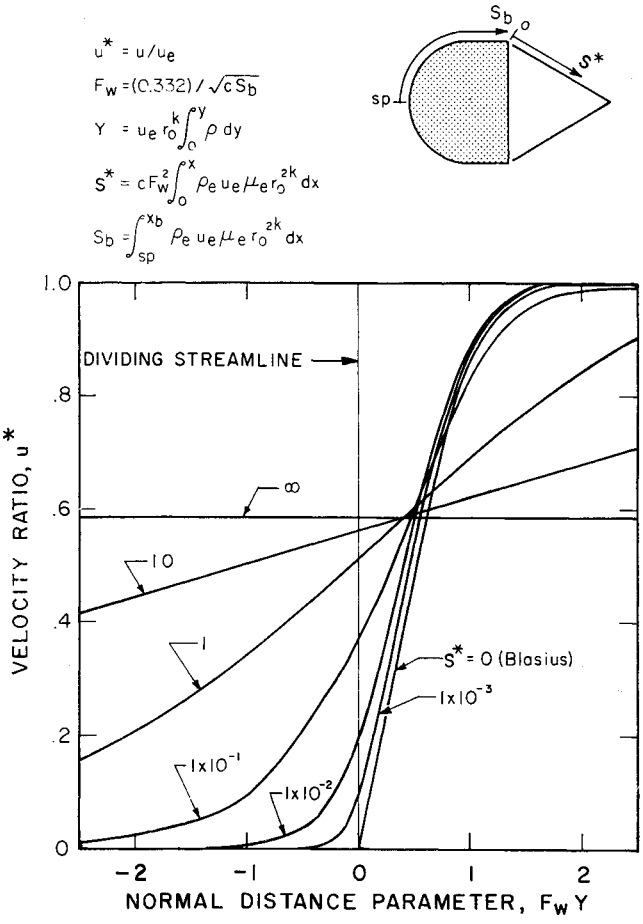

Fig. 6 Velocity profiles in terms of normal distance parameter

$u^* = u/u_e$

$S^* = cF_w^2 \int_0^x \rho_e u_e \mu_e r_0^{2k} dx$

$F_w = (0.332)/\sqrt{cS_b}$

$S_b = \int_{sp}^{x_b} \rho_e u_e \mu_e r_0^{2k} dx$

$\eta = Y/\sqrt{2cs} = F_w Y/\sqrt{2s^*}$

$Y = u_e r_0^{2k} \int_0^Y \rho dy$

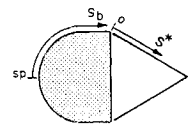

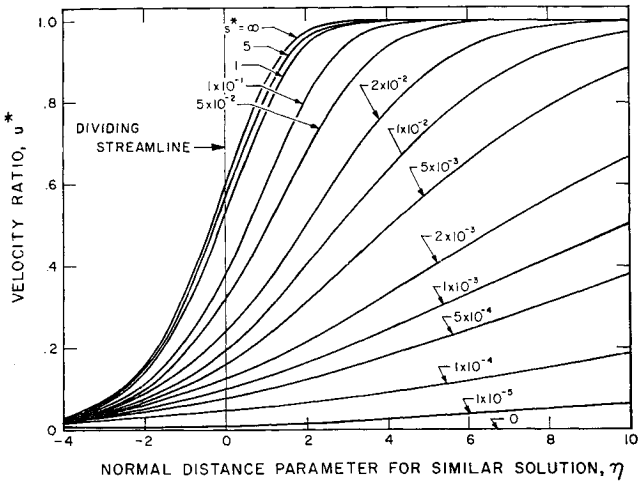

Fig. 7 Velocity profiles in terms of similarity parameter

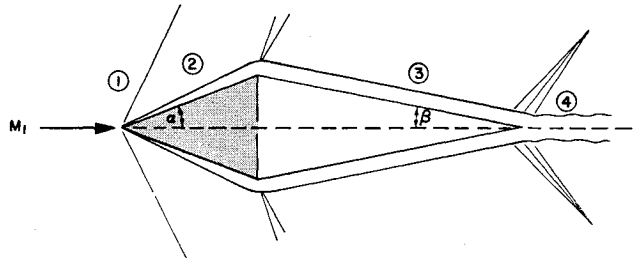

Fig. 8 Body geometry for ideal, constant γ, gas calculations

distribution. This led to difficult matrix inversion problems and the method was abandoned in favor of a finite difference method.

An implicit finite difference method such as that described in Ref. 8 was used. In the implicit method, the stability of this type of numerical integration is improved by using S^* centered finite difference approximations for derivatives with respect to u^*. The approximations used are

$$\partial F^*/\partial S^* = [F^*_{i,j+1} - F^*_{i,j}]/\Delta s^* \tag{21}$$

$$\partial F^*/\partial u^* = [F^*_{i+1,j+1} + F_{i+1,j} - F^*_{i-1,j+1} - F^*_{i-1,j}]/4\Delta u^* \tag{22}$$

$$\partial^2 F^*/\partial u^{*2} = [F^*_{i+1,j+1} + F^*_{i+1,j} - 2F^*_{i,j+1} - 2F^*_{i,j} + F^*_{i-1,j+1} + F^*_{i-1,j}]/2(\Delta u^*)^2 \tag{23}$$

where

$$i = u^* \text{ index}$$
$$= S^* \text{ index}$$

Eq. (13) becomes

$$F^*_{i-1,j+1} + J(i,j)F^*_{i,j+1} + F^*_{i+1,j+1} = H(i,j) \tag{24}$$

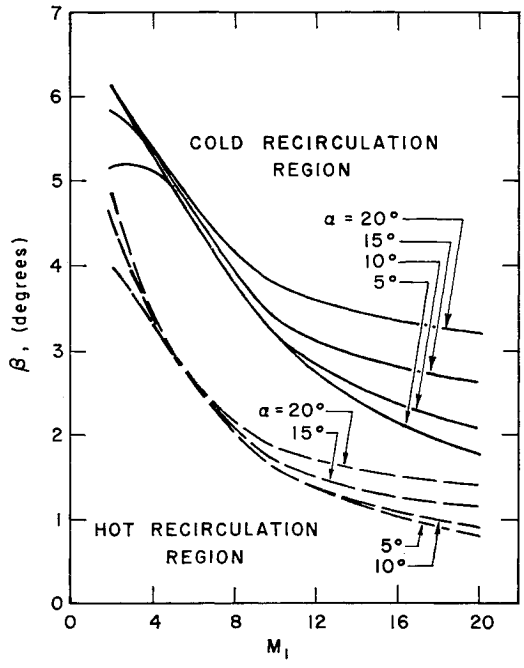

Fig. 9 Wake angle, β, for cones, $\gamma = 1.4$

$$J(i,j) = -2\left[1 + \frac{(i-1)(\Delta u^*)^3}{F^{*2}\Delta S^*}\right] \tag{25}$$

$$H(i,j) = -F_{i-1,j} + 2\left[1 - \frac{(i-1)(\Delta u^*)^2}{F^{*2}\Delta S^*}\right] F^*_{i,j} - F^*_{i+1,j}$$

Boundary conditions are

$$F^*_{i=1} = F^*_{i=N+1} = 0 \qquad N = 1/\Delta u^* \tag{26}$$

This equation can be written for $i = 2 \ldots N$, giving $N - 1$ coupled equations in $N - 1$ unknowns. The equations are evaluated by using

$$F^* = [F^*_{i,j} + F^*_{i,j+1}]/2 \text{ in } J(i,j) \text{ and } H(i,j) \tag{27}$$

The solution of the equations is repeated until the next mean value of F^* agrees within a prescribed tolerance with the previous value. The $N - 1$ equations are solved using the

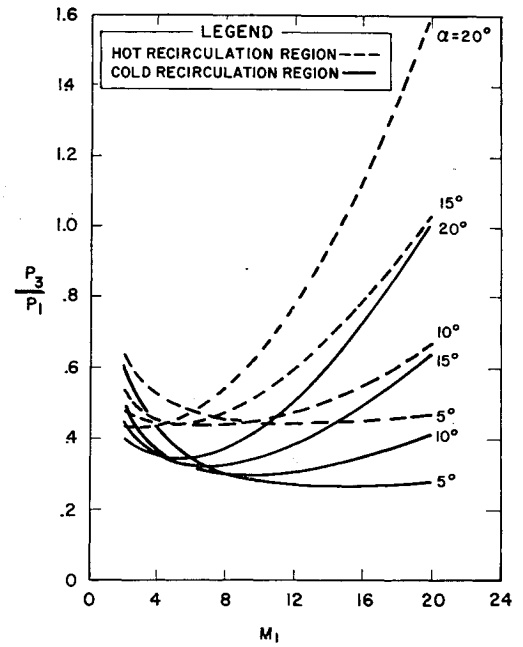

Fig. 10 Pressure ratio, P_3/P_1, for cones, $\gamma = 1.4$

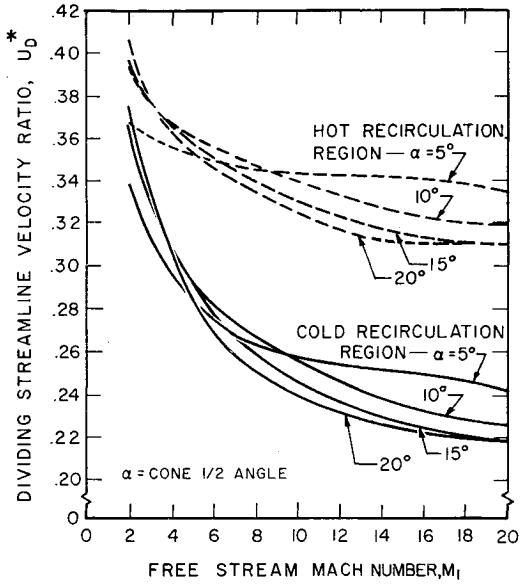

Fig. 11 Dividing streamline velocity ratio, u_D/u_3, for cones, $\gamma = 1.4$

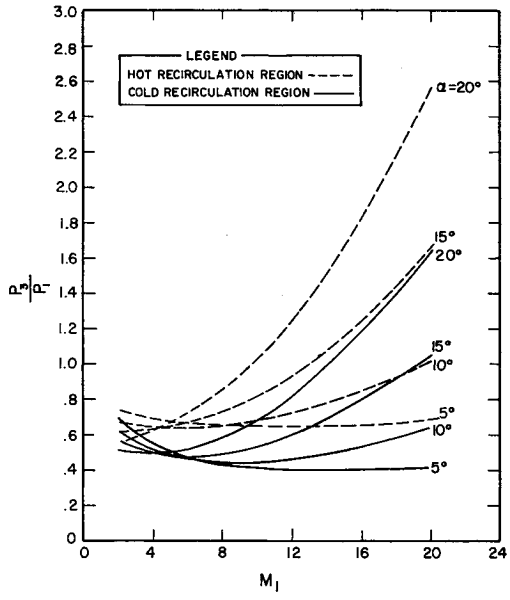

Fig. 13 Pressure ratio, P_3/P_1, for wedges, $\gamma = 1.4$

equivalent of Gaussian elimination.[8] The calculations were programmed for solution on an IBM 1620 computer, using 160 meshpoints in u^*.

VI. Results

The change of the shear function (vs velocity) profile with distance from the separation point at the base of the body is shown in Fig. 3. The maximum value of the shear function is reduced by an order of magnitude by the time S^* becomes 4. As is to be expected, with increasing S^*, the profile approaches the similar profile which assumes zero initial free shear layer thickness. This can be shown more clearly by plotting the similar shear function $f''(\eta)$ or $(2S^*)^{1/2}F^*$ vs u^* (Fig. 4). The similar profile is that labeled $S^* = \infty$. It is clear from this figure that if the distance, S^*, from the separation point at the base of a hypersonic body to the stagnation point at the rear of the recirculation region is smaller than that given by a value of the order of unity, the use of the similar profile is no longer justified.

The velocity at the dividing streamline is given as a function of the reduced distance S^* in Fig. 5.

The normal distance parameter YF_w vs velocity profile is given as a function of S^* in Fig. 6.

The approach of this profile to the similar velocity profile can be seen by plotting the similar normal distance parameter η or $YF_w/(2S^*)^{1/2}$ vs velocity (Fig. 7).

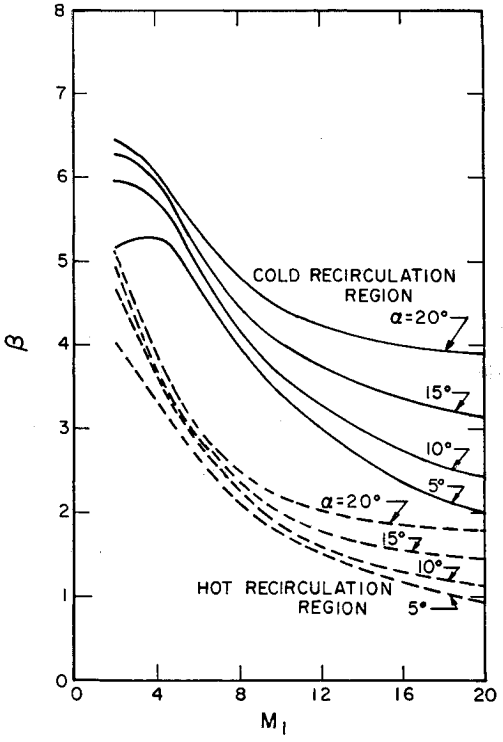

Fig. 12 Wake angle, β, for wedges, $\gamma = 1.4$

VII. Wake Angle and Base Pressure Calculations

In order to demonstrate the effect of these results on wake angle and base pressure calculations, a series of calculations was performed using an ideal, constant γ, gas. While the model is realistic at high Mach numbers only for small angle

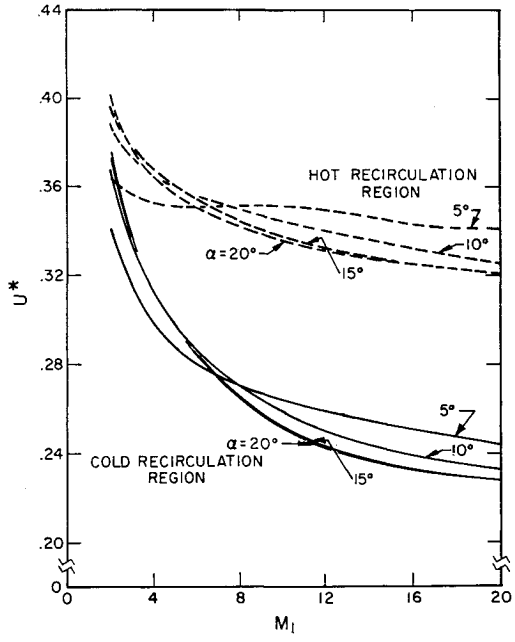

Fig. 14 Dividing streamline velocity ratio, U_D/U_3, for wedges, $\gamma = 1.4$

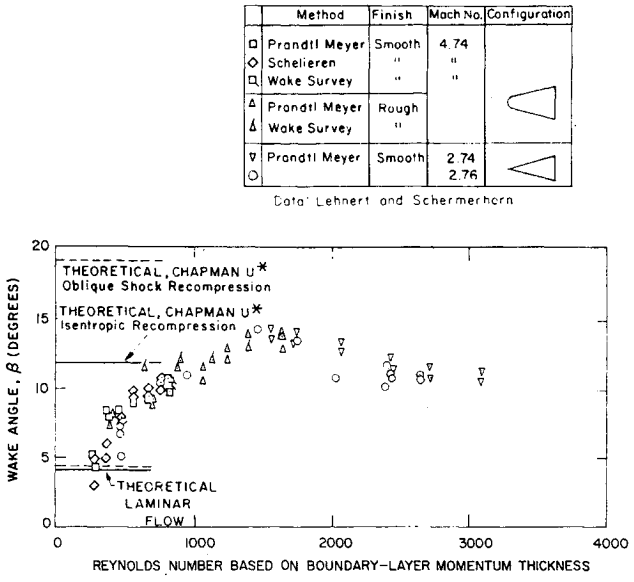

Fig. 15 Experimental wake angles, β

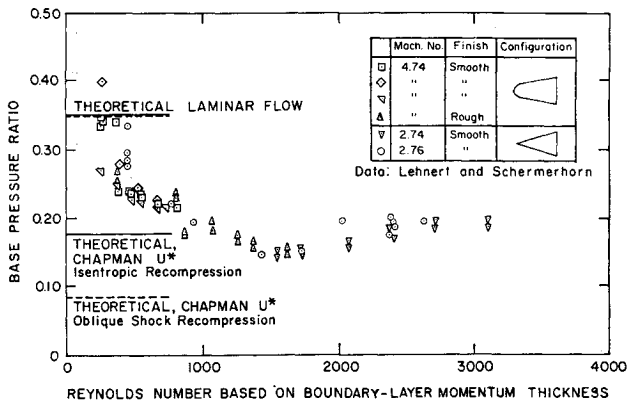

Fig. 16 Experimental pressure ratios, P_3/P_2

cones and wedges, the calculations were carried out to $M = 20$ for larger angles in order to illustrate the trend of behavior. A sketch of the body is shown in Fig. 8. Calculations were performed for both wedges and cones. The inviscid flow, just outside the boundary layer, was assumed to be described by a bow shock (oblique shock for a wedge, conical for a cone), a Prandtl-Meyer expansion from region 2 to region 3, and between regions 3 and 4, either an isentropic compression or an oblique trailing shock. These two assumptions as to the nature of the compression between regions 3 and 4 are believed to bracket the actual behavior. The inviscid flow equations give the pressure behind the trailing shock as a function of β, the wake angle. A second set of equations which also gives P_4 as a function of β is obtained from the assumption that the recompression region at the rear of the recirculation is small in extent and the total pressure on the dividing streamline is recovered at the rear stagnation point and is equal to P_4. These equations are

$$\frac{P_4}{P_3} = \left[1 + \frac{(\gamma - 1)}{2} M_3^2 \left(\frac{u_D}{u_3}\right)^2 \frac{T_3}{T_D}\right]^{\gamma/(\gamma-1)} \tag{28}$$

$$\frac{T_D}{T_3} = \frac{T_c}{T_3}\left(1 - \frac{u_D}{u_3}\right) + \left(1 + \frac{(\gamma - 1)}{2} M_3^2\right) \times \frac{u_D}{u_3} - \frac{(\gamma - 1)}{2} M_3^2 \left(\frac{u_D}{u_3}\right)^2$$

where the subscript D denotes properties on the dividing streamline, c denotes properties in the core of the recirculating region, and 3 denotes the inviscid flow just outside the free shear layer; u_D/u_3 can be obtained from Fig. 5 if S^* is known. For a wedge or cone, $csF_w^2 = (0.332)^2(CS/C_bS_b)$. For $C = C_b$, this becomes, from the definition of S,

$$S^* = \frac{\rho_3 u_3 \mu_3 \sin\alpha}{\rho_2 u_2 \mu_2 \sin\beta} (0.332)^2 \tag{29}$$

The value of β for which the value of P_4 calculated by each of the two methods is the same is the wake angle. The results of these calculations are given in Figs. 9–14. Only results assuming isentropic recompression are shown, since the difference between these curves and those for oblique shock recompression is appreciable only at low Mach numbers.

The sensitivity of these results to the value of the temperature of the core of the recirculating region is immediately apparent. The two extremes shown on the graphs correspond to the freestream stagnation temperature (hot) and freestream temperature (cold).

Lehnert and Schermerhorn[9] experimentally investigated the base pressure and wake angle of 10° half angle cones with no heat transfer and correlated them with the Reynolds number based on boundary layer momentum thickness. The freestream Mach number was sufficiently small (2.75) that a constant $\gamma = 1.4$ approximation is valid. They also investigated spherical nosed cones having the same local Mach number on the surface at the downstream end of the cone, and found that the base pressure and wake angle of these models correlated well with those of the sharp cones. Their results are given in Figs. 15 and 16. The values of the wake angle and base pressure ratio calculated using the value of u_D/u_3 given by Fig. 5 and those calculated using the limiting value of u_D/u_3 (0.587) are also shown in these figures.

Since the calculations are based on a laminar flow model, the measured data should approach the calculated values with decreasing Re_θ. The calculated values of pressure ratio and wake angle seem to agree well with the data.

VIII. Conclusions

The conversion of a Blasius profile to a Chapman distribution in the free shear layer has been successfully demonstrated. The range of validity of the Chapman profile is determined by means of the parameter S^*. If S^* is less than the order of unity, the calculations presented herein should be used to determine dividing streamline velocity, base pressure, wake angle, trailing shock strength, and throat size. Further investigations are required in order to determine the implications of these results on the downstream wake.

It is interesting to note that S^* is independent of Reynolds number and depends primarily on body shape and Mach number. This means that the base pressure, wake angle, and dividing streamline velocity near the neck should be independent of Reynolds number. However, the thickness of the free shear layer does depend upon Reynolds number. It would appear, therefore, that as long as the base of the body is large compared to the thickness of the shear layer the Reynolds number independence should hold for laminar flow. When the shear layer is thick it probably cannot be uncoupled from the internal recirculating region as it was in this paper.

Calculations presented in this paper have shown the sensitivity of the results of base flow calculations to the value of the temperature of the core of the recirculation region. In addition to the effect of the free shear layer inside boundary conditions on calculations of gross base flow properties such as wake angle and base pressure ratio, these conditions are also needed to change the results presented in this paper from transformed coordinates to physical coordinates. In general, in order to make this change, it is necessary to solve the energy and species conservation equations, and the proper choice of inside boundary conditions for these equations is open to question and should be investigated further.

The mathematical techniques used in this investigation appeared to work well and the extension of these calculations to the case in which there is blowing on the body surface—e.g., due to ablation—appears to be straightforward. In this case, the profiles of Emmons and Leigh[10] would be substituted for the Blasius profile.

Appendix: Free Shear Layer with Finite Chemical Rates

In order to change the solution of the momentum equation from reduced coordinates to physical coordinates, it is necessary, in general, to solve the energy and species conservation equations. These equations can be written

$$\rho\left(u\frac{\partial Ki}{\partial x}+v\frac{\partial Ki}{\partial y}\right)=\frac{\partial}{\partial y}\left(\frac{\mu}{\mathrm{Pr}}\,Le\,\frac{\partial Ki}{\partial y}\right)+W_i \qquad \text{species conservation}$$

where

K_i = mass fraction of species i

W_i = mass generation rate of species i

Here it has been assumed that diffusion is due to gradients in species concentration only and that all diffusion coefficients are equal.

$$\rho\left(u\frac{\partial h_S}{\partial x}+v\frac{\partial h_S}{\partial y}\right)=\frac{\partial}{\partial y}\left(\frac{\mu}{Pr}\frac{\partial h_S}{\partial y}\right)+\frac{\partial}{\partial y}\left(\frac{\mu}{Pr}\,[Pr-1]\frac{\partial u^2/2}{\partial y}\right)+\frac{\partial}{\partial y}\left(\frac{\mu}{Pr}\,[Pr-1]\times\sum_i\left\{\int_0^T C_{pi}\,dT+h_i{}^0\right\}\frac{\partial Ki}{\partial y}\right)$$

where

$$h_S=\sum_i K_i\left[\int_0^T C_{pi}dT+h_i{}^0\right]+\frac{u^2}{2} \qquad \text{energy conservation}$$

The assumption is now made that $Le = Pr = 1$ and the same transformations are made as were used for the momentum equation, resulting in the set of equations

$$u_*\frac{\partial F}{\partial CS}-F^2\frac{\partial^2 F}{\partial u_*{}^2}=0 \qquad \text{momentum}$$

$$u_*\frac{\partial K_i}{\partial CS}-F^2\frac{\partial^2 K_i}{\partial u_*{}^2}=\frac{W_i}{C\rho\rho_e u_e{}^2 r_0{}^{2k}\mu_e} \qquad \text{species}$$

$$u_*\frac{\partial h_S}{\partial CS}-F^2\frac{\partial^2 h_S}{\partial u_*{}^2}=0 \qquad \text{energy}$$

If the initial conditions are satisfied, the energy equation is satisfied by

$$h_S=h_{se}+u_*(h_{se}-h_{ic}) \qquad \text{energy}$$

where h_{ic} is the enthalpy in the recirculation region core, h_{se} is the enthalpy in the inviscid region just outside the free shear layer. These equations, along with the ideal gas equation and the rate equations making up W_i, permit the calculation of composition, temperature, density, and velocity profiles. The mathematical techniques used for the solution of the momentum equation should work equally well for the solution of the species conservation equations. There is some question as to the proper inner boundary conditions for these equations. In the case of pure air, it appears to be reasonable to assume that, since the velocity in the core of the recirculation region is small, the composition has time to reach equilibrium. However, the proper inner boundary conditions for contaminant species, such as one would get from ablation, are not known, and further study of this question is needed.

References

[1] Feldman, S., "On Trails of Axisymmetric Hypersonic Blunt Bodies Flying Through the Atmosphere," J. Aero. Sci. **28,** 433 (1961).

[2] Lees, L. and Hromas, L., "Turbulent Diffusion in the Wake of a Blunt-Nosed Body at Hypersonic Speeds," J. Aero. Sci. **29,** 976 (1962).

[3] Chapman, D. R., "Laminar Mixing of a Compressible Fluid," NACA TN1800 (1950); also "Theoretical Analysis of Heat Transfer in Regions of Separated Flow," NACA TN3792 (1956); also "An Analysis of Base Pressure at Supersonic Velocities and Comparison with Experiment," NACA TN2137 (1951).

[4] Lees, L., "Laminar Heat Transfer over Blunt-Nosed Bodies at Hypersonic Flight Speeds," Jet Propulsion **26,** 259–269 (1956).

[5] Moore, F. K., "On Local Flat-Plate Similarity in the Hypersonic Boundary Layer," J. Aero. Sci. **28,** 753 (1961).

[6] Goldstein, S., Proc. Cambridge Phil. Soc. **26,** 18 (1930).

[7] Dorodnitsyn, A. A., "Method of the Integral Relations for the Numerical Solution of Partial Differential Equations," Rept. Inst. Exact Mech. Computing Technique, Akad. Nauk SSSR (1958).

[8] Dewey, C. F., Schlesinger, S. I., and Sashkin, L., "Temperature Profiles in a Finite Solid with Moving Boundary," J. Aero. Sci. **27,** 59 (1960).

[9] Lehnert, R. and Schermerhorn, V. L., "Correlation of Base Pressure and Wake Structure of Sharp and Blunt-Nose Cones with Reynolds Number Based on Boundary-Layer Momentum Thickness," J. Aero. Sci. **26,** 185 (1959).

[10] Emmons, H. W. and Leigh, D., "Tabulation of the Blasius Function with Blowing and Suction," Div. of Applied Science, Combustion Aero. Lab., Interim Tech. Rept. no. 9, Harvard Univ. (1953).